ADVANCED MATERIALS
www.advmat.de

Inkjet Printing—Process and Its Applications

By *Madhusudan Singh, Hanna M. Haverinen, Parul Dhagat,* and *Ghassan E. Jabbour**

In this Progress Report we provide an update on recent developments in inkjet printing technology and its applications, which include organic thin-film transistors, light-emitting diodes, solar cells, conductive structures, memory devices, sensors, and biological/pharmaceutical tasks. Various classes of materials and device types are in turn examined and an opinion is offered about the nature of the progress that has been achieved.

1. Introduction

The organic electronics roadmap identifies organic and printed electronics market to exceed $300 billion over the next 20 years.[1] Print technology borrowed from the graphic arts and newspaper industry can be adapted in principle to the production of large volume organic electronics. In particular, digital inkjet printing, which has been used as a low cost research tool, is facilitating initial explorations of various aspects of printed electronics in a laboratory setting. The appeal of this technology lies in it being a non-contact, additive patterning and maskless approach. Direct write attribute of inkjet printing allows for deposition of versatile thin films, the designs of which can be changed with ease from batch to batch. Other attractive features of this technology are: reduced material wastage, low cost, and scalability to large area manufacturing.

In the sections that follow, we will attempt to present a brief overview of recent progress in the understanding of inkjet printing process (Section 2). A section on progress in organic thin-film transistors (Section 3) will be followed by a review of printed light-emitting devices (LEDs, Section 4). The development of economically viable solar cells requires high throughput processes, and inkjet printing provides an ideal capability for initial process development (Section 5). This will be followed by a summary of recent developments in printing of magnetic nanoparticles (Section 6) for memory and other related applications. All devices, organic thin film transistors (OTFTs), LEDs, and solar cells, require contacts and conductive structures (Section 7) as part of larger circuits that integrate them. Sensors and detectors are an integral part of many aspects of modern life, such as light detectors, safety, and security applications such as toxic gas sensors, etc. Many of these applications require inexpensive, often single-use devices that are ideally suited to inkjet printing. We will present a discussion of notable reports of progress in this field (Section 8). Finally, we will make a very brief survey of progress in printed biological and pharmaceutical devices and applications (Section 9), and the use of inkjet printing as a patterning process (Section 10), concluding with a concise summary. This Progress Report is not intended to be exhaustive in nature, but we choose particular applications of inkjet printing, which in our opinion, offer the greatest advance in their respective fields in recent years, and most promise for forthcoming work of a significant nature.

2. Inkjet Printing Process

Inkjet printing is a material-conserving deposition technique used for liquid phase materials. These materials, or inks, consist of a solute dissolved or otherwise dispersed in a solvent. The process essentially involves the ejection of a fixed quantity of ink in a chamber, from a nozzle through a sudden, quasi-adiabatic reduction of the chamber volume via piezoelectric action. A chamber filled with liquid is contracted in response to application of an external voltage. This sudden reduction sets up a shockwave in the liquid, which causes a liquid drop to eject from the nozzle. This process has been analyzed at some length and the reader is referred to recent review papers.[2] The ejected drop falls under action of gravity and air resistance until it impinges on the substrate, spreads under momentum acquired in the motion, and surface tension aided flow along the surface.[3] The drop then dries through solvent evaporation,[4] as shown in Figure 1. Recent studies[5] show that drop spreading and the final printed shape strongly depend on the viscosity, which in turn is a function of the molar mass of the polymer. More interestingly, the aforementioned group also found a printing height dependence of the final dried-drop diameter, which was a function of the polymer concentration.[6]

[*] Prof. G. E. Jabbour, Dr. M. Singh, P. Dhagat
School of Materials, Arizona State University
Tempe, AZ 85287 (USA)
E-mail: jabbour@asu.edu
Prof. G. E. Jabbour, Dr. M. Singh
Advanced Photovoltaics Center, Arizona State University
Tempe, AZ 85287 (USA)
Prof. G. E. Jabbour, H. M. Haverinen
Flexible Display Center, Arizona State University
Tempe, AZ 85284 (USA)
H. M. Haverinen
Optoelectronics and Measurement Techniques Laboratory
Department of Electrical and Information Engineering
University of Oulu
Oulu 90014 (Finland)

DOI: 10.1002/adma.200901141

Most conventional understanding of the inkjet printing process depends on assuming the flow of the fluid ink as a Newtonian fluid. This assumption is often invalid, especially in the case of the ''rebound'' of a fluid upon impact on a printing substrate with low surface energy. Bartolo et al. developed an understanding of the interaction of a non-Newtonian fluid with the substrate as a function of normal stress at the contact line between the fluid and the substrate.[7] They demonstrated that the rebound of the drop can be controlled or even prevented through addition of a small amount of flexible polymer to the solvent.

The flow properties of dilute polymer solutions are of immediate interest for the development of inkjet printing processes. Measurements such as contact angle presented by a single drop on the substrate of interest, coupled with a measurement of the viscosity, surface tension, and computational fluid dynamics modeling using software such as Fluent (ANSYS), have been used to study the flow process as well as interaction of a falling drop with the substrate. However, such an approach is necessarily approximate as it lacks direct measurements of fluid flow patterns, which can be critical for printing applications. Hill et al.[8] have introduced a rheofluorescent technique for the study of fluorescent polymers in a shear field. The method involves the investigation of dependence of fluorescence from poly[2-methoxy-5-(2′-ethyl-hexyloxy)-(1,4-phenylene vinylene)] (MEH-PPV) in a Couette flow situation between two cylinders, which rotate relatively to generate a shear force. Rheochromism, which involves a shift in the fluorescence peak depending on the applied shear force in a fluid, is studied to infer changes in segment length in the conjugated polymer. Polymer segment length, which is directly related to the molecular weight and, hence, viscosity, has a critical impact on the flow properties in piezoelectric inkjet printing, a situation that does involve compression of the fluid and shearing prior to its ejection from the nozzle. While this technique does not offer a direct handle on the actual flow pattern, it permits the study of the relationship between the optimal shear stress and the molecular weight of the species being printed.

Direct imaging offers a more direct measurement of ink flow patterns. The development of such a technique has been reported by Dong et al.[9] Here, a drop-on-demand (DOD) piezoelectric inkjet printing system was used in conjunction with a pulsed laser and a flash photography setup to obtain sufficient brightness in the field of view as well as good time resolution for direct imaging measurements of the drops. Several fluids, including DI water, glycerin-based mixtures of water, and isopropyl alcohol were used to measure the processes of ejection and stretching of fluid, necking and pinch-off of liquid streaks from nozzle, recoil of the freely falling liquid streak, breakup of the streak, formation and breakup of primary drop and satellites, stretching of the liquid drop, etc. The authors developed criteria for avoiding the formation of satellite drops that are responsible for reduction of resolution in the printing process. A less sophisticated method of reliably measuring the dried-drop size, which affects the morphology of the final print, involves the use of silica nanoparticles[10] in order to map the spreading of the drop and relate dried-drop size to the size of the sessile drop.

Inkjet printing depends critically on the behavior of ejected printed drops after the jetting action. These falling drops are affected by several factors including jetting conditions and properties of the ambient. Tsai et al.[11] studied the effects of pulse voltage on droplet breakup time from the nozzle, droplet morphology, drop velocity, and droplet size of silver nanoparticles dispersed in DI water, using pure DI water as control. They found that: (i) more viscous ink had a higher onset bias and created a longer liquid column and small droplets; (ii) by applying intermediate bias to both inks, two droplets were generated after jetting but they recombined before hitting the surface; (iii) higher voltages resulted in separated droplets that never recombined; (iv) break-off time is independent of the pulse bias; and (v) the pinch-off point for both solutions was different, where silver powder suspensions had lower pinch-off point compared to those of bare DI water.

In most cases, fabrication of functional device structures with inkjet printing involves the use of prepatterned substrates at multiple levels of processing, and potentially (in many cases) involving multiple materials. Such situations result in more complicated fluid flow patterns when compared to the simple case of a printed drop impinging on a flat substrate. Modeling of interaction of printed drop with a prepatterned surface has been treated by Khatavkar et al.[12] The authors used a diffuse interface model to consider the effect of wettability of the barrier and width of the barrier. Not surprisingly, the results indicated that for constant barrier geometry, wettability of the barrier is critical to determination of spreading of the printed drop.

Printing of thin lines is limited by the size of the drop, which depends ultimately on jetting conditions, the ink, surface energy of substrate, and nozzle diameter. Intuitively, the nozzle diameter should form the fundamental lower bound on the drop size, barring any unusual jetting conditions. Machining of smaller nozzles in inkjet cartridges is possible but it involves more complicated processes, thereby increasing cost. Further, smaller nozzles are easier to clog, thereby reducing the reliability and repeatability of the jetting process. Hence, the development of a printing process that can produce features smaller than the nozzle diameter is desirable. Such a process has been demonstrated by Goghari and Chandra[13] for water–glycerin

Ghassan E. Jabbour is the director of the Advanced Photovoltaics Center at Arizona State University (ASU), a director of research optoelectronic materials and devices at the Flexible Display Center (FDC), and a Professor of the School of Materials at ASU. He attended Northern Arizona University, MIT, and University of Arizona. He received his bachelor's degrees in Physics, Electrical Engineering, and Materials Science and Engineering. Prof. Jabbour is a SPIE fellow and a Distinguished Prof. of Finland, Academy of Finland. His research interests are flexible and stretchable electronic materials, energy, nanoelectronics, and photonics.

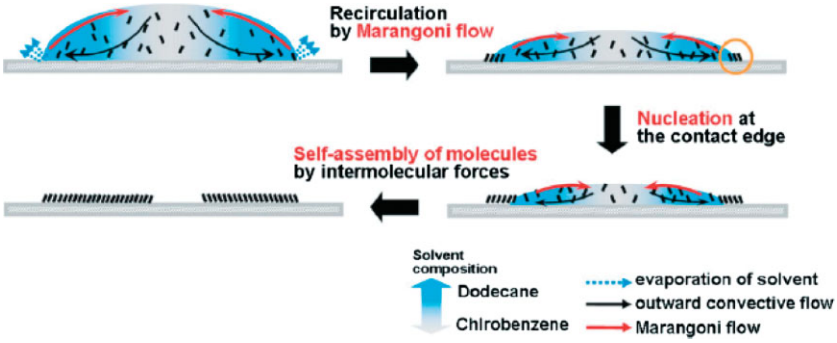

Figure 1. The process of drop drying after deposition with inkjet printing. Reproduced with permission from [4]. Copyright 2008, Wiley-VCH.

mixtures with intermediate concentrations. They developed a custom drop generator that exploits fluid instability to form small droplets. This instability depends on the material parameters satisfying certain conditions. The authors found that the Ohnesorge number,

$$\mathrm{Oh} = \frac{\mu}{\sqrt{\rho d \sigma}} \tag{1}$$

where μ, ρ, and σ are the viscosity, density, and surface tension of the ink, while d is the nozzle diameter, is a good predictor of when such conditions are satisfied.

At high integration densities, such as for electrophoretic backplanes, the tolerances online non-uniformities can be very tight. Thus, it is desirable to directly control the nature of the interaction between the ink and substrate. The coffee-ring effect, for instance, arises in part from interaction of multiple effects of drying of the solvent, resultant changes in the viscosity of the ink, transport of the solute via motion of the solvent, the latter motion arising from surface tension interaction between the solvent and the substrate, etc. It would be advantageous to arrest the final geometry and layout of ink drops on the substrate in a very short period of time after deposition. Use of thermally gelating polymers is one method that can help ensure this outcome. Printing of continuous polymer lines using gelating polymers has been demonstrated by van den Berg et al.[14] The authors used a diblock copolymer poly(vinyl methyl ether)-block-poly(vinyloxy-4-butyric acid) colloidally stabilizing a TiO_2 ink. Thermally gelating materials exhibit strong temperature dependence. The authors found a temperature-dependent increase in ink viscosity, which increased dramatically above 37 °C, along with the corresponding increase in print fidelity for printed drops and lines.

Other methods to increase resolution of printed features involve bypassing thermal/acoustic printing altogether and use electric fields to drive the printing process. An electrohydrodynamic jetting (EHJ) technique to achieve sub-micrometer resolutions was developed by Park et al.[15] resulting in feature sizes in the range of 240 nm to 5 μm. The reader is referred to this paper for more details on printing processes that involve the use of very high electric fields to propel ink drops, forming a Taylor cone at the tip of the capillary. An application of this approach to biological systems will be presented in Section 9.

Polymers and other solutions and suspensions lend themselves readily to inkjet printing. Fabrication of structures that involve species other than polymers or small molecules/macromolecules that are easily dissolved in solvents presents a new set of challenges. For instance, suspensions of metal nanoparticles tend to be unstable in ordinary solvents and can require complicated chemical modifications that involve use of stabilizers. Printed nanoparticles behave differently from printed polymers and other solutions owing to their higher specific gravity and increased likelihood for phase separation. The final assembly of such nanoparticles on the substrate depends on surface treatments which change surface energy properties. Perelaer et al.[10] investigated packing of inkjet printed spherical silica nanoparticles. The study involved four different nanoparticle sizes stabilized with hydroxyl or silanol surface groups in a 1 wt % aqueous solution. Using different surface treatments, the authors found that larger particles packed closer to the center of the droplet when the contact angle was high, while smaller particles under the same conditions migrated closer to the contact line at the edge of the droplet. Furthermore, the use of highly hydrophobic substrates assisted in packing of nanoparticles, avoiding coffee-ring formation.

Inkjet printing of homogenous polymer solutions is common. However, the use of colloidal suspensions expands the repertoire of polymer/solvent combinations that can be printed. This ability is particularly vital in designing a pure inkjet printing-based process to fabricate multiple layers with orthogonal solvents. Printing of aqueous inks containing a 40 wt % polyurethane suspension in water was demonstrated by van den Berg et al.[16] Using white light interferometry, the authors found that use of higher solute contents reduces print non-uniformities that arise from the coffee-ring effect.[3] The height of the single drop deposited was found to be 3 μm, while printing of a complete layer revealed a thickness of 10 μm. The authors also attempted to print a step structure resulting in a pyramid with a height of 87 μm.

We have thus attempted to address the gamut of features and issues unique to the inkjet printing process. These involve the measurement of rheological properties of the inks, droplet–substrate interactions, post-jetting behavior of printed droplets in flight and after collision with the substrate. We have briefly surveyed recent work on methods used to enhance the resolution of device structures composed of polymers and metallic nanoparticles. We now turn to various applications of inkjet printing.

3. Thin-Film Transistors

A key active element for implementing organic circuits is the OTFT. Use of OTFTs has been demonstrated in low-end applications, which do not require significantly high mobility and switching speeds, such as RFID tags[17] and display backplanes.[18] We will now discuss significant accomplishments in the area of printed organic transistors. We will focus on both all-printed and hybrid devices (where conventional lithography is

used in conjunction with printing). An OTFT is a four-layer device with two layers of electrode material (source, drain, and the gate) and one layer each of dielectric and active organic material. Although the basic structure of an OTFT appears simple, complexity arises due to registration and solvent orthogonality issues with layer-by-layer printing. These problems can be compounded when printing on nonplanar substrates, as the case for flexible electronics. Additionally, the switching speed of a circuit depends upon mobility and the channel length (L) to channel width (W) ratio of the transistor. In most cases, inkjet printing offers a resolution $\geq$20 μm,[1] but limits the smallest channel length that can be achieved. This has implications on the circuit design, limiting the switching speeds to 1–100 Hz.[19]

Most of the recent efforts have been focused on reducing the channel length in order to overcome the switching speed limitation. Sirringhaus et al.[20] successfully demonstrated the use of a hybrid approach to create channel lengths from the micrometer to sub-100 nm range. They used lithographically patterned hydrophobic polyimide banks to contain the spread of inkjet printed source–drain (S/D) electrodes on a hydrophilic glass substrate[20] creating channel features with ~5 μm separation. Further reduction in the channel lengths was possible using e-beam lithography to pattern a hydrophobic self-assembled monolayer (SAM) mesa-like structure, which varied in width from 20 μm to 250 nm. Surface energy differences between the mesa and the substrate split an inkjet-printed droplet into two separate S/D electrodes with the length of the channel being defined by the width of the SAM mesa.[21] Furthermore, they demonstrated the use of nanoimprint lithography to create trenches in polymethyl methacrylate (PMMA) with a separation of 250 nm (which defined the channel length) in order to confine printed droplets.[22] For devices mentioned above, poly(3,4-ethylenedioxythiophene):poly(styrenesulfonate) (PEDOT:PSS) was used as the S/D electrode material. The organic semiconductor and the dielectric material were spin-coated, and finally the gate electrode (PEDOT:PSS) was printed on top of the dielectric layer with a registration accuracy of 1 μm, to complete the device.

However, the use of conventional lithography tools is expected to lead to an increase in production cost. A more cost-effective approach based upon self-aligning electrodes, resulting in 100 nm channel lengths, was developed.[23] This technique requires inkjet printing first set of PEDOT:PSS electrodes and treating them with a carbon tetrafluoride (CF_4) plasma to create a hydrophobic surface. Next, a second set of PEDOT:PSS electrodes are printed partially overlapping the first set. Ink from the second print is repelled from the first set of electrodes, before drying in the vicinity forming a sub-100 nm self-aligned gap (SAG) between the two electrodes. Additive printing of organic semiconductor and gate electrode complete the device, with solvent being the only material wasted. Use of this approach resulted in transistors with mobility values of 0.002 $cm^2\ V^{-1}\ s^{-1}$ with poly(9,9-dioctylfluorene-*co*-bithiophene) (F8T2), a liquid crystalline polymer. The authors also demonstrated that addition of a surfactant to the PEDOT:PSS ink also created a self-aligned separation between printed electrodes. The hydrophilic tail groups from the surfactant accumulate on the surface of the drying droplet due to segregation of the surfactant to the surface. This creates a low-surface tension layer surrounding the droplet, which repels the second printed droplet. More recently, they were able to a combine the SAG with a high mobility organic semiconductor poly(2,5-bis(3-dodecylthiophene-2-yl)thieno[3,2-b]thiophene) (pBTTT) to obtain respectable mobility values of 0.1–0.2 $cm^2\ V^{-1}\ s^{-1}$. However, in this case, printed gold electrodes ($\sigma = 10^4$ S cm^{-1}) treated with a hydrophobic SAM were used to repel the second printed electrode to resulting in channel lengths from 60 nm to 4 μm. Inverters based on these transistors exhibited frequencies as high as 1.6 MHz.[19]

In order to fabricate all-printed OTFTs, the dielectrics have to be compatible with the inkjet processing of subsequent layers. Orthogonal solvents are required in order to prevent dissolution of layers that have been previously printed. Despite the difficulties in ensuring these conditions, all-printed transistors have been demonstrated using pentacene precursors and poly-4-vinylphenol (PVP) dielectric;[24] and polypyrrole and PVP-K60.[25] Additive printing of active layer inks (organic semiconductors dissolved in various solvents) such as poly[5,5′-bis(3-dodecyl-2-thienyl)-2, 2′-bithiophene] (PQT-12),[26] F8T2,[27] air-stable poly(3-hexylthiophene) (P3HT) derivatives,[28] 6,13-bis(triisopropylsilylethynyl) pentacene (TIPs pentacene),[29] other pentacene precursors and oligothophenes[30] have been demonstrated. Recently, carbon nanotubes (mobility ~ 0.07 $cm^2\ V^{-1}\ s^{-1}$) have been inkjet printed as the active material for OTFTs.[31] Other inorganic species such as polysilicon[32] and zinc oxide nanoparticles[33] have also been successfully inkjet-printed as active layers in a transistor. Electrode materials such as PEDOT:PSS, silver nanoparticle inks, gold and copper nanoparticle inks have been utilized as potential candidates.[28,34–37]

Next, we focus on using inkjet printing as a digital lithography tool in order to create masks such that the minimum printable feature size defines the channel length of the device. The PARC group has demonstrated the use of wax as a photoresist to lithographically define S/D electrodes pattern on blanket metal thin films.[27,38] Areas that are covered by the wax are protected from subsequent lithographic processes such as metal etching and photoresist removal. The drop size is controlled by temperature of both wax and substrate, resulting in channel lengths ranging from 40 to 400 μm. Digital lithography using wax has been used to define all the three electrodes in a coplanar bottom gate OTFTs and has been successfully used to create backplanes for electrophoretic displays using PQT-12 as the active material. This resulted in mobility values of 0.06–0.2 $cm^2\ V^{-1}\ s^{-1}$ for channel lengths of 30–50 μm.[26] The same group demonstrated similar performance with a printed backplane[39] consisting of silver nanoparticle lines with a resistivity of $5 \times 10^{-6}\ \Omega$ cm. We will address the printing of such conductive structures at greater length in Section 7. Printed wax has not only been used to define critical devices features but also used for selective patterning process.[40] On a substrate with predefined S/D electrodes, the channel region is covered with wax after which the substrate is exposed to SAM making the uncovered area hydrophobic. The wax is then removed exposing the hydrophilic region underneath it. The substrate is dipped in an organic polymer solution and gradually removed to allow for selective dewetting of the solution from the hydrophobic regions onto the hydrophilic areas. This simple patterning of organic semiconductor layer offers good registration between successive layers.

The accurate placement of the active material within the gate electrode region prevents large leakage currents and crosstalk

between TFT pixels, as well as conserves ink. Recently, Lim et al.[4] demonstrated use of solvent mixtures to balance the Marangoni and convective flows in a drying droplet, thereby controlling morphology of the dried droplet (Fig. 2). The evaporation rate is controlled using a high surface tension and high boiling point solvent (major solvent) mixed with a lower boiling point solvent (minor solvent) and surface tension less than that of the major component. A convective flow is established from the center toward the drying edge of the droplet as the evaporation rate is faster at the periphery; driven by the surface tension gradient between the edge of the drop and the center. However, this surface tension gradient creates an opposing Marangoni flow, which results in recirculation of the solvent in the droplet. The dried droplet then resulted in large self organized crystals of TIPs pentacene which provided mobility as high as 0.12 cm^2 V^{-1} s^{-1}.

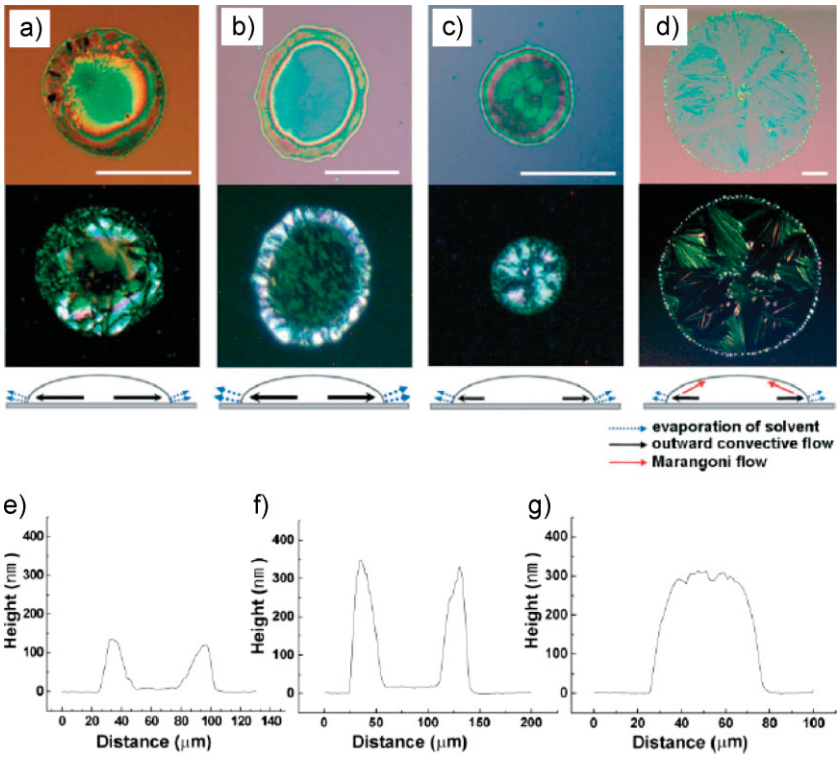

Figure 2. Optical microscopy and polarized images of the inkjet-printed droplets of TIPS pentacene using chlorobenzene as the major solvent mixed with 25% of the minor solvent, a) chlorobenzene, b) hexane, c) *o*-dichlorobenzene, and d) dodecane. (Scale bar represents 50 μm) The profilometery images of single dots using chlorobenzene mixed with 25% minor solvents, e) chlorobenzene, f) hexane, g) *o*-dichlorobenzene are also shown. Reproduced with permission from [4]. Copyright 2008, Wiley-VCH.

Inkjet printing of OTFTs has been limited to bottom contact architecture wherein the electrodes were S/D electrodes were deposited before the organic active layer. This prevented damage to the organic active layer from the ink solvent, preserving the device performance. Also, the registration issues were limited to the printing of gate electrode for top gate. Recently, there have been developments with top contact OTFT geometry, where the metal S/D electrodes are printed on top of the active layer.[41,42] Ability to control the drop volume to picoliter values, limited the amount of organic solvent dispensed on top of the active layer. Another advantage of reduced droplet volume was a decrease in sintering temperature for metallic nanoparticles that formed the electrodes preventing subsequent damage to the underlying organic layer. Continuous metallic lines as narrow as 1 μm with resistivity values of ~25 μΩ cm were obtained in this manner. Further details of this report will be presented in Section 7. Mobility obtained for pentacene OTFTs fabricated using printed electrodes was 0.1–0.3 cm^2 V^{-1} s^{-1}, which is comparable with those of evaporated electrodes. This technique was also demonstrated on an n-type semiconductor copper hexadecafluorophthalocyanine (F16CuPc) resulting in mobility values of 0.02 cm^2 V^{-1} s^{-1} ($L = 5$ μm). This also benefits the bottom contact geometry where much smaller feature sizes can be obtained without the use of conventional lithographic processes for miniaturization of printed circuits.

High integration densities of field-effect transistors (FETs) and TFTs require device structures with a high capacitance per unit area to maintain proper control of the channel. Perovskites like $BaTiO_3$[43] and polar materials like $LiNbO_3$[44] can be used to enhance such control through enhancement of capacitance per unit area, in addition to more exotic polar effects such as charge induction. It is thus desirable to develop an inkjet printing technique for deposition of such materials accurately over the channel. Tseng et al.[45] demonstrated the deposition of $BaTiO_3$-Ni perovskite films through inkjet printing. The authors printed 60-nm-diameter $BaTiO_3$ nanoparticles, and 90-nm-diameter metallic nickel particles with purity >99% on flexible porous acetate sheets using a propylene glycol-based surfactant to disperse the nanoparticles in ethanol–isopropanol solvent blend.

However, before the commercialization of TFT and FET-based products, there are road blocks that require immediate attention and significant amount of work. Registration of features at different layers of print has to be resolved for high throughput inkjet printing. The solvents need to be compatible when printing subsequent layers and yet be environmentally safe for use in large scale production. Additionally, passivation of the printed device is also important for long lifetime operation capabilities. Recently, Arias et al.[46] have demonstrated the feasibility of using blended active and encapsulation material that phase separate upon printing in the channel region. There is limited exposure of the active polymer to ambient conditions during the print cycle and resulted in cost effective printing of both active and encapsulation layer in a single step.

4. Light-Emitting Devices

Inkjet printing does not require the use of shadow masks as it is a direct writing process. This property of inkjet printing makes it a suitable technique for combinatorial studies[47,48] of various

devices, including organic light emitting diodes (OLEDs). Optimization of OLED device structures often involves use of different device thicknesses, and determination of optimal device designs. This process often entails multiple experiments and repeated measurements of the electroluminescent properties of different devices, which is at once time-consuming and material intensive. Tekin et al.[49] used inkjet printing to examine the influence on the emission properties of six different poly-(phenylene-ethynylene)/PPV (PPE-PPV)-based π-conjugated polymers with different side chains and film thicknesses in a parallel manner. They found a strong dependence of the emission wavelength on inter-chain interactions, which in turn depend on both the chemistry and the device thicknesses. Photoluminescence of inkjet printed inorganic semiconductor nanoparticles was demonstrated by the same group[50] as part of a combinatorial study. An aqueous mixture of thioglycolic acid or 3-mercaptopropionic acid stabilized CdTe nanoparticles with 1 wt % polyvinyl alcohol (PVA) and varying glycol concentrations (0–20 vol %) was printed on ITO and glass. The authors observed that the best morphology and drop formation occurred with 2 wt % of glycol, suppressing the ring formation drastically. Smoother films were only formed when PVA was used in the mixture rather than printed separately. In order to investigate luminescence properties of the nanocrystals in embedded polymer matrix, PVA and poly(diallyldimethylammonium chloride) (PDDA) with different weight concentrations were printed and characterized with fluorescence spectroscopy. Photoluminescence study showed strong emission when dots were embedded in PVA but weakened emission in the case of PDDA (Fig. 3). This method in principle can be used for other devices, such as organic solar cells, OTFTs, etc. and considerably reduce the process, environmental variations, and resulting uncertainties involved in sequential processing of different device structures.

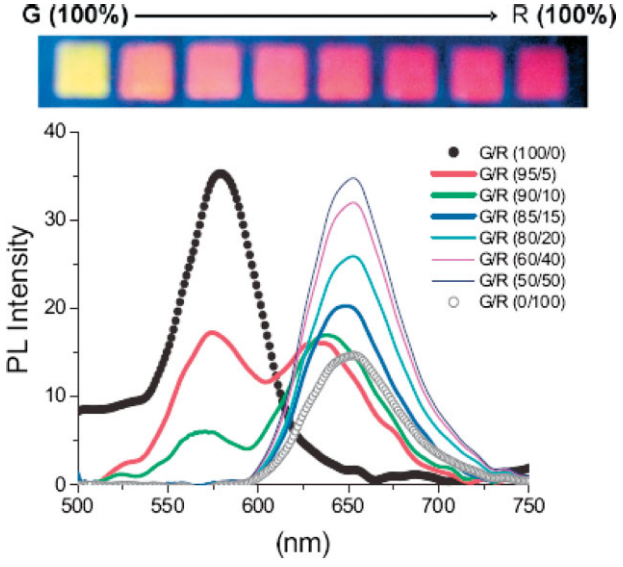

Figure 3. Combinatorial study of printed red and green nanoparticles. The top part reveals a color change from green to red with various red–green NP mixtures. The PL spectra on the bottom refer to the same library. Reproduced with permission from [50]. Copyright 2007, Wiley-VCH.

Singh et al.[51] demonstrated bright inkjet printed OLEDs based on Ir-based phosphorescent macromolecules anchored on a polyhedral oligomeric silsesquioxane (POSS) molecular scaffolding used as a phosphorescent dye in a polymer ink containing a hole transporting polymer, poly(9-vinylcarbazole) (PVK) and an electron transporting polymer, 2-4-biphenylyl-5-4-tertbutyl-phenyl-1,3,4-oxadiazole (PBD). The authors achieved a peak luminance of more than 6000 cd m^{-2}, a relatively low turn-on voltage (6.8 V for 5 cd m^{-2}), and a quantum efficiency of 1.4%. White light interferometry measurements revealed large interface roughness (51 nm) for the printed layers, which underscores the role of suitable ink chemistry in determining overall device brightness, in spite of quenching from rough cathode contacts. Through improvements in dye chemistry and print morphology, the authors were able to achieve a peak luminance[52] of 10000 cd m^{-2} (Fig. 4).

Recently, Haverinen et al.[53] demonstrated electroluminescence from inkjet printed inorganic semiconductor nanoparticles embedded between spin coated hole transport polymer and a thermally evaporated organic small molecule electron transport layer. Octadecylamine stabilized CdSe/ZnS quantum dots (QDs) were dispersed in chlorobenzene and inkjet printed onto an optically cross-linked poly(*N*,*N*′-bis(4-butylphenyl)-*N*,*N*′-bis(phenyl)benzidine) (poly-TPD) layer under ambient conditions. Nearly a monolayer of the printed QDs was capped with a 1,3,5-tris(2-*N*-phenylbenzimidazolyl (TPBi) electron transport layer followed by the deposition of a LiF/Al cathode. ITO was used as the anode. Preliminary results showed an external quantum efficiency of 0.19% and brightness of 381 cd m^{-2} (at 15.9 V). Furthermore, the extension of inkjet of QDs to display applications was shown by printing on a prepatterned substrate having about 243 pixels of QVGA format, operating under common cathode. The study also demonstrated polycrystalline packing of the printed QDs layer surface. In addition, the study demonstrated simple control of the emitted color by optimizing the number of printed drops per pixel. In this regard, the pixel

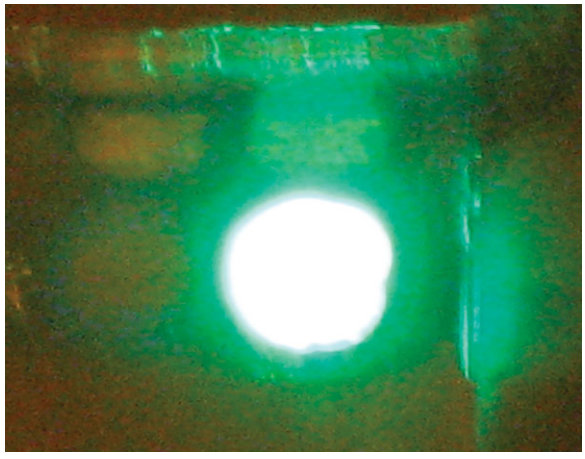

Figure 4. Photograph of a 10000 cd m^{-2} OLED printed using Ir-based POSS macromolecules emitting at a peak wavelength of 520 nm. The shape of the illuminated region of the device is not perfectly round due to slight printing non-uniformities. The bluish-white region arises from the saturation of the CCD camera at high brightness.

emission can be tuned from blue to orange due to a combination of emission from the QDs and the organic layers.

Single-wall carbon nanotubes (SWCNTs) are notoriously difficult to disperse uniformly in solvents and tend to form non-conductive mixtures due to aggregate formation. Shigematsu et al.[54] reported a custom-built electrostatic inkjet setup and demonstrated an ability to print aqueous SWCNT solutions. Jetting parameters were investigated as a function of solution viscosity. Nanotubes were dispersed in a water:isopropanol:glycol mixture. The printed layer was used as a cathode in a field emission setup, where ITO coated with a phosphor was placed 25 μm away from the cathode. Field emission was measured in vacuum (5×10^{-5} Pa) and resulted in an 8 μA current at 1100 V.

In contrast to LEDs, electrochromic devices exhibit large changes in observed color as a function of applied voltage. Small et al.[55] printed water soluble multi-wall carbon nanotube (MWCNT) in a polyaniline (PANI) composite with a 32% MWCNT loading factor. Nanotube dispersion with 10 mg mL^{-1} concentration was deposited on a polyethylene terephtalate (PET) substrate and resulted in a transmittance of 68% and sheet resistance ~5 kΩ sq^{-1}. Upon increasing the number of printed layers (from 1 to 3), transmittance dropped to ~30% with a decreasing sheet resistivity ~1.1 kΩ sq^{-1}. Furthermore, the printed layers showed electrochromic behavior. A nanotube/PANI blend was printed on gold coated polyvinylidene fluoride (PVDF) and platinum coated ITO substrates. With a variation of the potential between −0.2 and 0.8 V, the color changed from yellow to green, and ultimately to blue.

5. Solar Cells

Solar cells offer the promise of harnessing the Sun's energy to drive power systems, transportation systems, etc. Solar cells have not yet achieved widespread use owing to the unfavorable cost comparison against fossil fuel-based energy sources. This state of affairs is a result of: (i) more expensive materials, (ii) costlier processing methods, and (iii) relatively low efficiencies with the more cost effective solution processable materials such as organic small molecules and polymers. Ever since the initial demonstration of screen printed organic solar cells,[56] printing have been seen to offer the promise of developing industrially scalable cost effective processes.

Use of bulk heterojunction structures in inkjet printed solar cells has been shown to be effective by the Schubert and coworkers.[57,58] Hoth et al.[59] from Konarka Technologies Inc. used a blend of P3HT and PCBM in *o*-dichlorobenzene and mesitylene to demonstrate inkjet printed organic solar cells with a Ca:Ag top cathode on PEDOT:PSS coated ITO. They achieved fill factor of 64% coupled with short circuit currents of 8.4 mA cm^{-2} and an open-circuit voltage of 0.54 V with device power conversion efficiency (PCE) of 2.9%. More recently, Aernouts et al.[60] demonstrated inkjet printed polymer:fullerene blend solar cells (PCE = 1.4%) utilizing a blend of P3HT and PCBM in a 1:1 ratio. While the present efficiency values are not very high for commercial applications, the progress made thus far is promising.

Inkjet printing can be used to deposit materials for inorganic and hybrid organic/inorganic solar cells. $CuIn_xGa_{(1-x)}Se_2$ (CIGS) has been used as a material for high-efficiency solar cells.[61–63] However, the process has traditionally involved deposition from potentially toxic precursors in a low-volume, high cost fashion. While there exist material limitations for sustained availability of indium and gallium worldwide,[64] the absence of a cost-effective environmentally sound process has been a more serious short-term limitation in the way of more widespread use of this material for commercial CIGS solar cells. Nanosolar Inc.[65] has developed a nanoparticle ink consisting of CIGS and an inkjet process to print it. Other commercial interest in this technology comes from HelioVolt Inc.,[63] ISET,[66] and smaller companies in the US and Europe.

6. Memory and Magnetic Applications

The use of inkjet printing has been extended to magnetic data storage applications. Magnetic nanoparticles of iron oxide [(Fe_2O_3, γ-Fe_2O_3) and Fe_3O_4], 65–80 nm in diameter, were synthesized and subsequently inkjet printed by Voit et al.[67] In order to stabilize the nanoparticles, dextran or polystyrene coating was applied. Dextran coated particles were mixed into water and 50 wt % glycerol while polystyrene coated particles were dispersed in diprolylene glycol. Superconducting quantum interference device (SQUID) magnetometery measurements revealed a coercivity of 15 Oe at room temperature for dextran coated nanoparticles. Polystyrene coated particles dispersed in dipropylene glycol were reported to have similar magnetic properties. Ink was jetted using a Xaar piezoelectric printer (XJ128-360) onto glass, plastic, and paper substrates. Line widths of 40–200 μm were achieved. Further magnetic properties of ink jet printed films were investigated using magnetic force microscopy (MFM).

Inkjet etching of polymer microstructures was demonstrated by Schubert and coworkers.[16] In addition to etched structures of polystyrene with applicable solvents and etching of polystyrene/Cr/Au films, magnetic nanoparticles were deposited onto the periphery of etching droplet via migration of particles during droplet drying. Superparamagnetic magnetite particles (1 wt %) were dispersed in toluene, stabilized with lauric acid and printed. Detection of nanoparticles at the ring surface was executed with scanning force microscope. Further consideration of patterning using inkjet printing-based techniques is provided in Section 10.

7. Contacts and Conductive Structures

Metals and conductive polymers form the basis of contacts and interconnections necessary for the functioning of electronic circuits, which can be composed of building blocks like FETs, or serve as logic/backplanes for electro-optic devices (like LEDs and photovoltaics) and memory components. Conventional contacts and conductive lines are traditionally defined using lithography techniques. However, the maskless direct write property of inkjet printing can be used to define conductive lines of significant complexity. Though these structures typically involve printing of silver and gold nanoparticles, some of the presented references involve the use of mixed metal nanoparticles and conductive polymer nanoparticles as well as organometallic inks.

It has been mentioned previously that the coffee-ring effect is one of the major reasons for non-uniform film deposition. The same considerations apply to nanoparticle-based solutions, or

suspensions. Li et al.[68] studied drying conditions of silver nanoparticle droplets and morphological properties of films to determine a critical drying temperature, T_c, for optimal film formation. In this case silver nanoparticles (diameter 30 nm), suspended in ethanol, were first printed on glass slides and dried at different temperatures from 12 to 60 °C, and finally sintered in vacuum at 400 °C. The morphology of deposited films was determined using profilometer and found to be in good agreement with theoretical data, which predicted that by increasing drying temperature, film formation changed from hill-like to ring profile formation (see Fig. 5), resulting in poor film quality. In this work, T_c was shown to be strongly dependent on volume of the drop, varied between 300 pL and 10 μL, increasing with volume, as expected. High density integration, such as in backplanes, requires tight tolerances on the width of printed interconnects.

Effort toward optimized printed lines with silver ink has been an interest in various groups. Recently, van Osch et al.[69] reported a 40 μm line width for inkjet printed silver nanoparticle ink by using Dimatix materials printer equipped with a 1 pL nozzle, on substrates such as polyarylate, Teflon LP, Teflon A, PET, and Kapton. After sintering at 200 °C for an hour, silver line conductivity was measured to be 13–23% of bulk conductivity, which is 63×10^{-6} S m^{-1}. Further improvement for line widths on untreated substrates was recently demonstrated by Meier et al. They used a 10 pL nozzle, modified the nozzle waveform, and heated the cartridge and sample platen to 55 °C. The reported printed silver lines were 25 μm in width. DC resistance per unit length was measured for various layer thicknesses (1–3 layers) and ranged between 84 and 184 Ω cm^{-1}, being inversely proportional to line thickness.[70]

Gamerith et al.[37] printed electrodes made of Ag–Cu nanoparticles and an organometallic Ag precursor molecular species. They used a simple 2-point method to estimate the conductivity of silver in each case: 7.3×10^3 S cm^{-1} for the Ag–Cu nanoparticles and 1.7×10^5 S cm^{-1} for the pure silver electrodes. Gold nanoparticles can also be used for printing conductive structures. In order to reduce minimal possible line width, Zhao et al.[71] extended the use of a self aligned printing approach to printing gold nanoparticles (1–4 nm in diameter) in xylene/cyclohexylbenzene. Printed gold features with high conductivity ($\sim 2 \times 10^4$ S cm^{-1}) were reported.

Sekitani et al. successfully demonstrated sub-femtoliter inkjet printing of gold nanoparticles by employing an EHJ technique. The observed 1 μm resolution enabled short channel length TFT fabrication without any prior surface treatment or complicated patterning technique. Authors reported a relatively small contact resistivity (5 kΩ cm) as well as small parasitic capacitance (6 pF) and practical line resistivity of less than 25 μΩ cm.[41]

Seeking further improvements in the resolution of inkjet printed gold nanoparticle structures, Ko et al.[28] demonstrated a hybrid technique that combines printing with a selective laser sintering process. In this method, hexanethiol capped Au particles are first printed followed by Ar ion laser ($\lambda = 514.5$ nm) sintering, followed by a solvent wash to remove remnant unsintered particles. This technique results in uniform and high-resolution patterns with a 1–2 μm line width. Furthermore, inkjet printing of Au nanoparticles with lower sintering temperatures has been applied to plastic substrates. In this case,

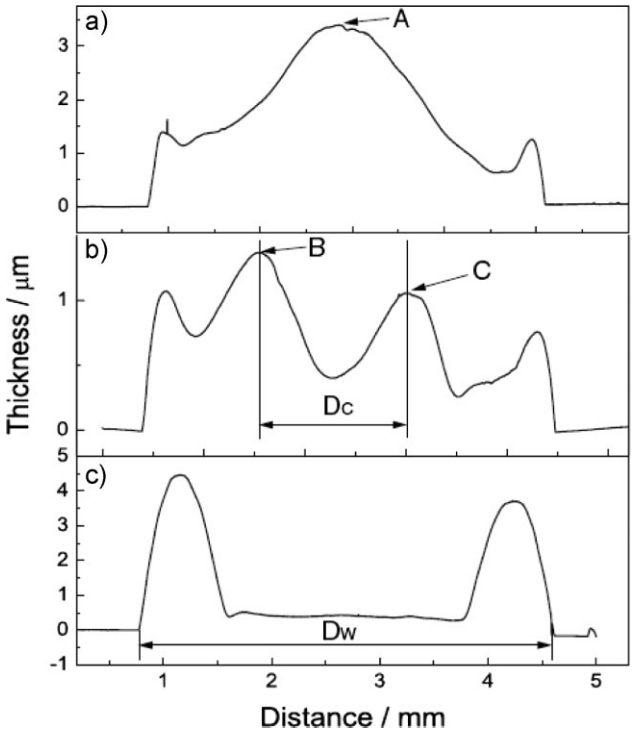

Figure 5. Cross-sections of droplets with changing drying temperatures reveals a formation change from a ''hill-like'' to a ''ring'' formation. Temperatures are a) 30, b) 35, and c) 60 °C, respectively. Reproduced with permission from [68]. Copyright 2007, The Japan Society of Applied Physics.

inkjet printed gold lines with 1 μm thickness had a sheet resistance of 0.03 Ω sq^{-1}, reducing conductivity to 70% of the bulk value.[72] The same group reported the inkjet printed radio frequency identification devices (RFIDs) by using Au nanoparticles. The use of polyimide dielectrics with Au nanoparticles in an inductor/interconnect multilayer structure yielded Q values of 0.5 at 135 kHz for a 1 μm thick conductor.[36]

Inkjet printing of aqueous nanodispersions of PANI nanoparticles was demonstrated by Ngamna et al.[73] Printing of these materials was possible upon optimization of surface tension and rheological properties of the spherical PANI dodecylbenzenesulfonic acid (PANI-DBSA) nanoparticles. Printed patterns using conductive PANI nanoparticles were shown proving the ability in depositing them with inkjet system. Furthermore, conductivity of printed films was reported as 4×10^{-4} S cm^{-1} (bulk) and is in good comparison with much thicker drop casted layer which had a conductivity of 8×10^{-4} S cm^{-1}. Particle size distribution was reported to be uniform, close to 82 nm in diameter.

Song et al.[74,75] studied the electrical properties of printed patterns of SWCNTs. SWCNTs of 5 nm diameter and 10 μm length were dispersed in dimethylforamide and printed on precleaned and plasma-treated glass as well as polymer substrates with various drying conditions. It was shown that faster drying (60 °C vs. room temperature) enabled a more even density distribution of the carbon nanotubes. Charge carrier properties were investigated for different line widths, from 170 to 1295 μm, which correspond to 1–8 overwriting steps, respectively. Resistance was shown to decrease, as expected, from 191 to

5.7 kΩ. Impedance analysis exhibited a similar trend: an increase in the number of printed layers resulted in a decrease in impedance values from 517 to 7.4 kΩ at 100 kHz. Based on their observations, these printed SWCNTs could be used in high frequency electronic devices due to the measured 10 MHz bandwidth in Ohmic characteristics.

As reported by Mustonen et al.[76] carboxyl functionalized SWCNT (SWCNT-COOH), and PEDOT:PSS/SWCNT-COOH composites patterns were fabricated by inkjet printing. In this case, they aimed at printing conductive and transparent films on photo paper, as well as on PET substrates. Nanotubes, 4–5 nm diameter and 0.5–1.5 μm long, were mixed with PEDOT:PSS and printed using a desktop printer (CanonBJC-4550), and a Dimatix DMP-2831 materials printer. Bare nanotubes on PET showed poor adhesion and high sheet resistance ($\rho > 4$ MΩ sq^{-1} at 50 prints). However, printed patterns on photo paper had reasonable sheet resistance ($\rho \sim 115$ kΩ sq^{-1} at 30 prints). On the other hand, for thick layers of composite ink versus just polymer ink, there was no significant difference in conductivity. Both films were shorted with sheet resistance about 1 kΩ sq^{-1}, and 70% transparency in the visible spectrum. Similarly, functionalized MWCNT (MWCNT-COOH) suspended in water[77] showed sheet resistivity values of 40 kΩ sq^{-1} (minimum of 30 prints) when printed on paper or plastic substrates.

Oyhenart, et al.[78] reported on fabrication of photonic bandgap structures using a conductive polymer (PANI: conductivity = 12 S cm^{-1}), with an inkjet printing process. They chose a relatively conductive polymer as conductive species like metals exhibit enhanced absorption at optical frequencies. With increase in the number of printed layers of the patterned structure, the authors found an increase in the transparency of the structure at well-defined frequencies up to 100 GHz. While this could be a result of multilayer interference, the authors claim this to be a signature of the onset of photonic bandgap behavior.

Inkjet printing can be employed at room temperature. Hence, it can address a larger class of chemical compounds, which, while being otherwise well-suited to desired device structures, cannot be deposited using more conventional deposition methods. Further, plastic-based electronics offer the prospect of using inexpensive and flexible substrates. Hiraoka, et al.[79] fabricated patterned thin films of conductive compounds: $BO_9(C_{14}\text{-TCNQ})_4$ (BO = bis ethylenedioxy tetrathiafulvalene and C_{14}-TCNQ = tetradecyltetracyano-quinodimethane) on 125 μm thick polyethylene naphthalate (PEN) base films. Inkjet printing was chosen as the deposition method as the compound is thermally unstable and cannot be deposited using thermal evaporative methods at elevated temperatures. The authors found an inverse linear dependence of the resulting sheet resistance of printed TCNQ derivatives on the number of printed layers (for $N > 3$, where N is the number of printed layers). Sheet resistances were close to 10^4 Ω sq^{-1} for more than 10 layers. The authors also fabricated pentacene transistors on these substrates and found fairly high mobilities ~0.21 cm^2 V^{-1} s^{-1} for top-contact and 0.12 cm^2 V^{-1} s^{-1} in bottom-contact geometry. Due to their intrinsically higher current densities, OLED applications typically require lower sheet resistances than the one found in this work. However, with appropriate selection of the material and proper design of the injecting contact, it is potentially possible to lower the injection barrier sufficiently, as well as reduce the voltage drop across the contact to use this technology in OLEDs and OTFT applications.

8. Sensors and Detectors

Sensors play an important role in industrial, transport security and safety-based applications. There are numerous classes of sensors including photodetectors, gas sensors, and mechanical stress sensors. In this section, we will examine different types of sensors fabricated using inkjet printing.

Nanoparticles composed of organic compounds can be used as organic active materials dispersed in aqueous solutions. Typical applications lie in food and drug industry, as well as cosmetics, but these special compounds have also been used in chemical catalysis in all kinds of application areas. Crowley et al.[80] introduced an ammonia sensor based on amperometric detection by using inkjet printed dodecylbenzene sulfonate (DBSA)–doped PANI nanoparticles on screen printed carbon electrode. Sensor response as a function of film thickness was investigated by printing one to four PANI layers. The sensitivity limit of this sensor was studied with a variety of different concentrations of ammonium chloride (0–80 μM) resulting in a calculated detection limit of 2.58 μM. Such sensor was reported to be stable within 15 days of testing period and with a response level of 1 mM (ammonium).

Development of aqueous-based inks of functional materials is of critical importance for inkjet printing applications. Success of such endeavors will allow a wider entry and adoption of inkjet technology. In this sense, a desktop inkjet can truly become a laboratory tool for materials discovery and device fabrication.[81] Along these lines, Jang[82] reported a convenient method for developing an aqueous dispersion of PANI-PSS nanoparticles and demonstrated their use as an inkjet printed ammonia sensor. The nanoparticles (diameter 30 nm) were synthesized using chemical-oxidation polymerization, dispersed in water and mixed with ethylene glycol and isopropyl alcohol to adjust the viscosity and surface tension prior to printing. The device structure consisted of a printed PANI-PSS film with various thicknesses and two copper electrodes. The sensitivity of the resulting sensor is shown in Figure 6. An ultralow concentration of 10 ppb was reported.

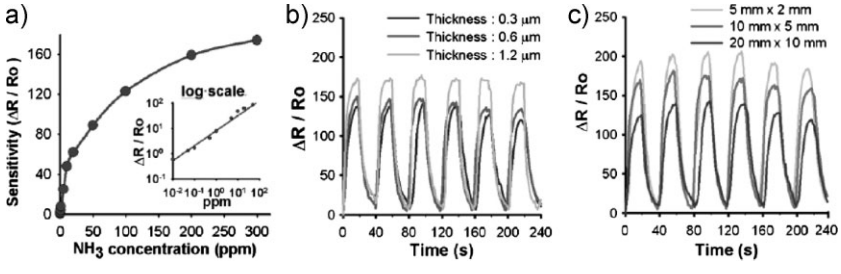

Figure 6. Sensitivity of PANI-PSS films as a function of NH3 concentration (a). Increasing thickness and decreasing sensing area has a positive impact on sensor sensitivity (b,c). Reproduced with permission from [82]. Copyright 2007, Wiley-VCH.

Börberl et al.[83] demonstrated a highly sensitive photodetector based on inkjet printed HgTe nanoparticles. At the room temperature, a detectivity of $D^* = 3.9 \times 10^{10}$ cm Hz^{12} W^{-1} at 1.4 μm wavelength was observed. HgTe crystals were dispersed in chlorobenzene (2 wt %) and printed on glass. The detectors were completed by evaporating interdigitated Ti/Au electrodes. Different printed nanocrystal layers were investigated in order to find sufficient film thickness to absorb incident light. A six layer device showed sensitivity of 65 mA W^{-1} at 10 V. It is worth noting that the sensitivity increased linearly, reaching 600 mA W^{-1} at 70 V. Interestingly, the authors reported demonstration of a detector for wavelengths up to 3 μm, which is remarkable considering that HgTe PL emission decreases significantly when emission wavelength is larger than 2 μm (Fig. 7).

Panhuis et al.[84] used coiled conformation biopolymers to distribute SWCNTs and printed transparent composite films on a PET substrate. They found very low conductivity when measured under a nitrogen atmosphere (current was reported below the sensitivity of the measurement apparatus). Surprisingly, they found that the resistance of the composite fell to ~12 MΩ when the film was exposed to ambient. The resistance of a biopolymer film with similar geometry as the composite one was 350 MΩ under ambient conditions. The change in conductivity is attributed to a change in the pathways in the nanotube–biopolymernanotube junctions in presence of water vapor due to mechanical swelling of the biopolymer matrix (Fig. 8). However, the presence of water vapor can also enhance conductivity due to presence of aqueous electrolytes when exposed to the ambient. The authors do not consider this or other candidate explanations for observed behavior. Regardless of the origins of this conductivity enhancement, it is possible to use this printed device as a humidity sensor.

For some applications, micro-electromechanical system (MEMS)-based sensors involve the deposition of functional layers to perform chemical and biochemical sensing tasks. Bietsch et al.[85] demonstrated the fabrication of nanoscale cantilever-based sensors using inkjet printing. SAM layers of alkanethiols were deposited on gold-coated cantilever structures. These SAM layers enhance the sensitivity of the cantilevers to ionic concentrations and pH in liquids. The authors used a similar approach for detection of gene fragments—by coating the cantilevers with thiol-linked single strand DNA oligomers. They reported a method to additively build three-dimensional MEMS and electrical circuitry by ink-jet printing nanoparticle Au metal colloids.

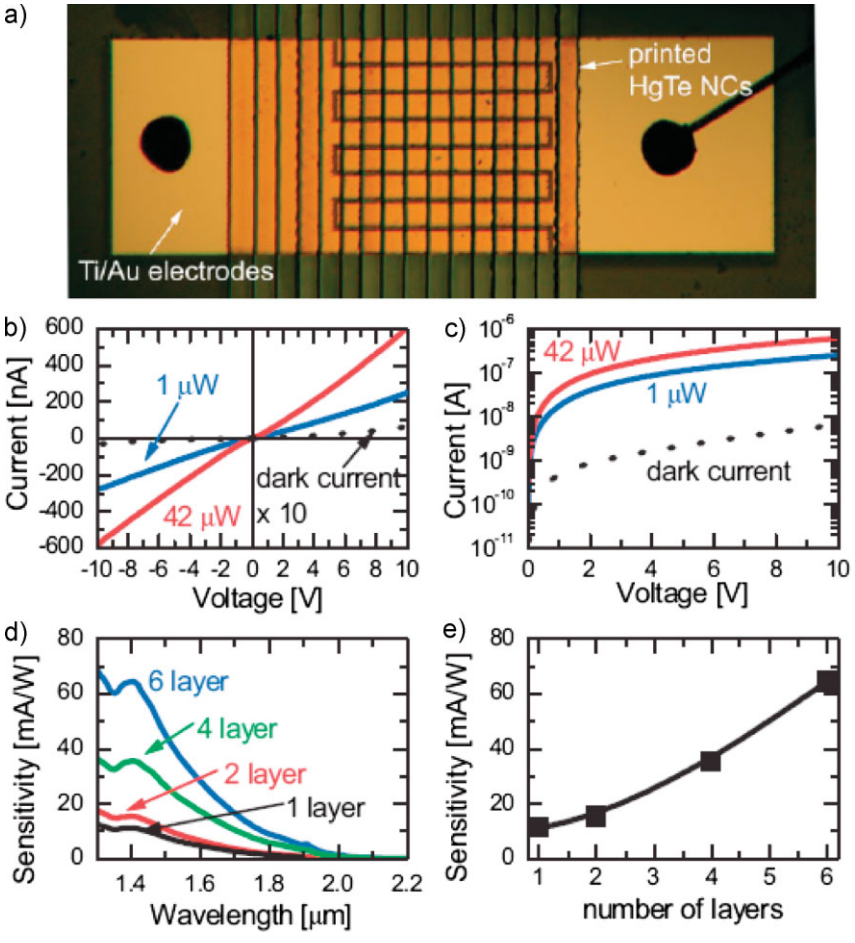

Figure 7. a) 16 HgTe nanocrystal stripes with interdigitated electrodes. Linear and logarithmic IV characteristics of the 6 layer photodetectors with 1 and 42 μW (b,c). Sensitivity of the detectors increases as a function of increasing printed layers (d,e). Reproduced with permission from [80]. Copyright 2007, Wiley-VCH.

9. Biological and Pharmaceutical Applications

Vesicles in the nanometer size range are used extensively in biomedical applications such as drug screening, and in living cells, play an important role in secretory processes such as endocytosis and exocytosis. Hauschild et al.[86] demonstrated a method to print these entities into a liquid solution. The assembly of vesicles proceeds from the printing of precursors called amphiphiles into a solution. The introduction of minute, controlled quantities of such precursors is important for fabrication of reproducible vesicles of tightly defined size and shape. Since it involves a printing process, this can be scaled to an industrial level. To achieve smaller dispensed drops of living systems, Jayasinghe et al.[87] used EHJ to form droplet deposits a few micrometers in size for formation of colloidal suspensions. The authors used Jurkat cells, as well as a variety of living human cells for this experiment and found no evidence that the exposure to high electric fields was harmful to the deposited living systems. The literature on the application of printing technologies to drug testing, rapid prototyping, and pharmaceutical research is vast and well beyond the scope and intent of this work. The reader is directed to a review on the subject by Yu et al. [88] and a recent article on bio-printing by Derby.[89]

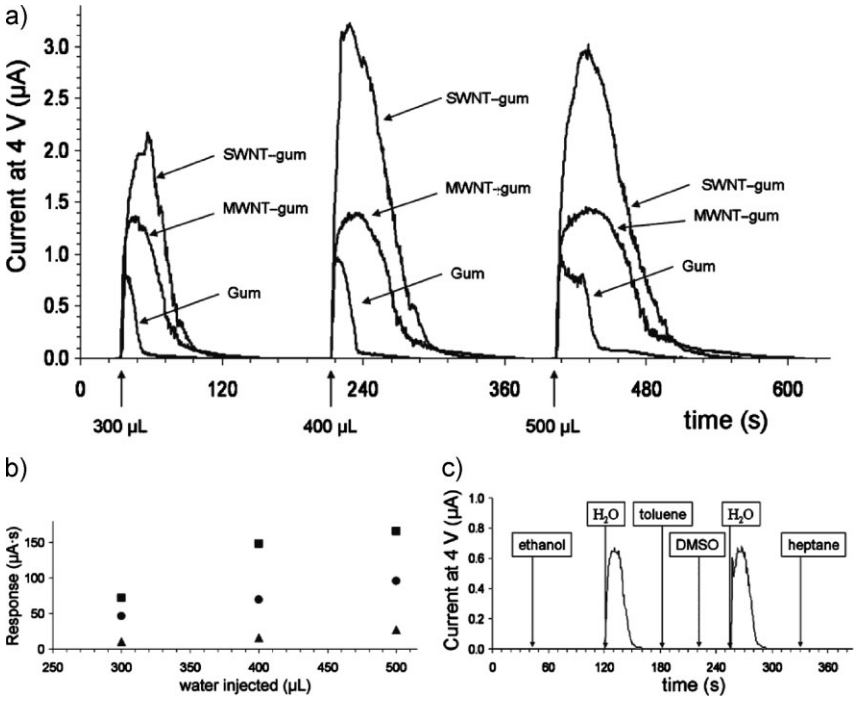

Figure 8. Response to water vapor with various printed film compositions are shown in (a,b). Nanotube-gellan gum dispersion is hypothesized to lead to better responsivity due to better conductivity. c) Printed MWCNTs and gellan gum films show no response to organic compounds Reproduced with permission from [81]. Copyright 2007 Wiley-VCH.

10. Inkjet Patterning

It has been stressed before that the use of inkjet printing obviates the need for conventional lithography in deposition of printed layers. It is thus appropriate at this point to consider the inverse of this, such as use of inkjet printing as a patterning or as an etch-dispensing process. Such use of inkjet printing is beneficial in situations that involve the removal of very small fraction of a predeposited material, such as in etching of isolation dielectrics in the multi-step standard CMOS process.[90]

Inkjet printing offers resolutions in the micrometer range, and hence it is a potential technique for dispensing etching species, in applications like flat-panel displays, etc. The ability to integrate various elements through inkjet printed interconnects and vias was demonstrated by Kawase et al.[91] An insulator layer of PVP was successfully etched by printing drops of ethanol. They demonstrated inverter circuits with frequencies of 250 Hz. More recently, Xia and Friend[92] demonstrated such a patterning technique by printing solvent drops onto a spin-coated insulator layer to form OLEDs. They used ethanol as a solvent, printed on to a layer of PVP, and reported devices with a brightness of around 800 cd m^{-2}. While conservation of OLED materials was not the focus of this work, it nevertheless demonstrates flexibility in processing offered by use of inkjet printing as an etching tool. de Gans et al.[93] have also demonstrated similar capabilities. They studied the dependence of via radius on the number of printed drops, as well as widths of etched grooves on the density of printed drops, and found good agreement between theory and experiment. Generally, wet etching is known to have a lower resolution than the commonly used dry etching processes, such as reactive ion etching.[94] However, in the case of polymer layers, dry etching processes are often too aggressive, leaving wet etching methods as a viable solution to the fine etching problem for these systems. Use of inkjet printing to dispense etch solvent helps to simplify the wet etching process, bypassing the lithographic mask definition, exposure and development steps. However, much work is needed on several fronts including shrinking patterning dimensions, minimizing clogging of nozzle region, and others, before inkjet can be adopted in a wide range of microelectronics manufacturing.

11. Summary

Materials deposition processes for OTFTs, OLEDs, solar cells, etc. currently involve the use of either spin-coating or vacuum deposition approaches; in a few cases inkjet printing was utilized to deposit one or more layers of the device structure. Unlike inkjet printing, traditional deposition approaches involve a great deal of wasted material, but result in a fairly uniform deposition profiles over the substrate. By contrast, inkjet printing is an anisotropic (localized) deposition process that lends itself readily to patterned writing/maskless processing. Given the inherent cost of lithography steps in industrial manufacture and the imperative to reduce the number and level of complication of such steps, inkjet printing provides an attractive, material-conserving alternative for several patterning applications. However, the anisotropic nature of inkjet printing also gives rise to issues not encountered in planar processing currently used in industry. The tendency of dissolved polymers and other nanoparticle species in solutions and suspensions to form coffee-ring-like structures is an inevitable effect of the surface-tension-driven transport of solutions along a surface with an evaporating solvent. Significant progress has been achieved in recent work to minimize the impact of such drawbacks on film uniformity and device performance. Incomplete coverage due to coma formation during spin-coating on prepatterned substrates can be obviated through the use of a patterned deposition process such as inkjet printing. In closing, inkjet printing is also a suitable process in situations where deposition of a given material must occur in predetermined locations on a substrate having pre-existing structures and devices that would, otherwise, be contaminated and/or damaged if a vacuum or spin-coating process were used. Given the impressive recent progress and extension of inkjet printing to novel areas of materials deposition, we anticipate a strong future for this technology in applied science and engineering.

There is significant scope for wider industrial application of inkjet printing technologies. Current trends in research applications of inkjet printing yield the first impression that the use of the technology may have peaked. However, current work using

inkjet printing across various applications suggests that the focus has been on uniformity and two-dimensional coverage of substrates. A better understanding of the flow properties of interacting droplets with the substrate or previously deposited layers is likely to open up possibilities for study of better controlled growth in the vertical dimension. With suitable technological advancements, the minimum amount of fluid dispensable can be further reduced. This reduction can be used to attempt the deposition of SAMs from very dilute solutions with long printing times, deposition of optically active thin layers for non-linear optics (NLO) and OLED applications, superlattices for hybrid PVs incorporating low-dimensional systems such as QDs. Use of EHJ-based techniques has recently acquired great interest, and further developments in this field are likely to address the issue of minimum resolutions achievable with printing. A great deal of work remains to be done in fundamental understanding of the fluid flow process during inkjet printing to facilitate further advances in this very exciting field.

Acknowledgements

M.S. and G.E.J. would like to acknowledge funding from Nitto Denko Technology and Advanced Photovoltaics Center. G.E.J. would like to thank FUJIFILM Dimatix, Inc. for theirsupport. P.D. and G.E.J. acknowledge funding from the Army Research Laboratory under the Cooperative Agreement W911NG-04-2-0005. G.E.J. and H.M.H acknowledge the FiDiPro program and the Graduate School of Modern Optics and Photonics, Finland.

Received: April 3, 2009
Published online: August 25, 2009

[1] *OE-A Roadmap for Organic and Printed Electronics*, Organic Electronics Association OE-A, Frankfurt, **2008**.
[2] E. Tekin, P. J. Smith, U. S. Schubert, *Soft Matter* **2008**, *4*, 703.
[3] D. Pesach, A. Marmur, *Langmuir* **1987**, *3*, 519.
[4] J. A. Lim, W. H. Lee, H. S. Lee, J. H. Lee, Y. D. Park, K. Cho, *Adv. Funct. Mater.* **2008**, *18*, 229.
[5] J. Perelaer, P. J. Smith, E. van den Bosch, S. S. C. van Grootel, P. H. J. M. Ketelaars, U. S. Schubert, *Macromol. Chem. Phys.* **2009**, *210*, 495.
[6] J. Perelaer, P. J. Smith, M. M. P. Wijnen, E. van den Bosch, R. Eckardt, P. H. J. M. Ketelaars, U. S. Schubert, *Macromol. Chem. Phys.* **2009**, *210*, 387.
[7] D. Bartolo, A. Boudaoud, G. Narcy, D. Bonn, *Phys. Rev. Lett.* **2007**, *99*, 174502.
[8] E. K. Hill, R. L. Watson, D. E. Dunstan, *J. Fluoresc.* **2005**, *15*, 255.
[9] H. Dong, W. W. Carr, J. F. Morris, *Phys. Fluids* **2006**, *18*, 072102.
[10] J. Perelaer, P. J. Smith, C. E. Hendriks, A. M. J. van den Berg, U. S. Schubert, *Soft Matter* **2008**, *4*, 1072.
[11] M. H. Tsai, W. S. Hwang, H. H. Chou, P. H. Hsieh, *Nanotechnology* **2008**, *19*, 335304.
[12] V. V. Khatavkar, P. D. Anderson, P. C. Duineveld, H. H. E. Meijer, *Macromol. Rapid Commun.* **2005**, *26*, 298.
[13] A. A. Goghari, S. Chandra, *Exp. Fluids* **2008**, *44*, 105.
[14] A. M. J. van den Berg, A. W. M. d. Laat, P. J. Smith, J. Perelaer, U. S. Schubert, *J. Mater. Chem.* **2007**, *17*, 677.
[15] J.-U. Park, M. Hardy, S. J. Kang, K. Barton, K. Adair, D. K. Mukhopadhyay, C. Y. Lee, M. S. Strano, A. G. Alleyne, J. G. Georgiadis, P. M. Ferreira, J. A. Rogers, *Nat. Mater.* **2007**, *6*, 782.
[16] A. M. J. van den Berg, P. J. Smith, J. Perelaer, W. Schrof, S. Koltzenburg, U. S. Schubert, *Soft Matter* **2007**, *3*, 238.
[17] A. Dodabalapur, *Mater. Today* **2006**, *9*, 24.
[18] J. Jang, *Mater. Today* **2006**, *9*, 46.
[19] Y.-Y. Noh, N. Zhao, M. Caironi, H. Sirringhaus, *Nat. Nanotechnol.* **2007**, *2*, 784.
[20] H. Sirringhaus, T. Kawase, R. H. Friend, T. Shimoda, M. Inbasekaran, W. Wu, E. P. Woo, *Science* **2000**, *290*, 2123.
[21] J. Z. Wang, Z. H. Zheng, H. W. Li, W. T. S. Huck, H. Sirringhaus, *Nat. Mater.* **2004**, *3*, 171.
[22] J. Z. Wang, J. Gu, F. Zenhausern, H. Sirringhaus, *Appl. Phys. Lett.* **2006**, *88*, 133502.
[23] C. W. Sele, T. Werne, R. H. Friend, H. Sirringhaus, *Adv. Mater.* **2005**, *17*, 997.
[24] S. E. Molesa, S. K. Volkman, D. R. Redinger, A. de la Fuente Vornbrock, V. Subramanian, *IEEE Int. Electron Device Meeting Tech. Digest* **2004**, 1072.
[25] Y. Liu, K. Varahramyan, T. Cui, *Macromol. Rapid Commun.* **2005**, *26*, 1955.
[26] A. C. Arias, S. E. Ready, R. Lujan, W. S. Wong, K. E. Paul, A. Salleo, M. L. Chabinyc, R. Apte, A. S. Robert, Y. Wu, P. Liu, B. Ong, *Appl. Phys. Lett.* **2004**, *85*, 3304.
[27] K. E. Paul, W. S. Wong, S. E. Ready, R. A. Street, *Appl. Phys. Lett.* **2003**, *83*, 2070.
[28] S. H. Ko, H. Pan, C. P. Grigoropoulos, C. K. Luscombe, J. M. J. Frèchet, D. Poulikakos, *Nanotechnology* **2007**, *18*, 345202.
[29] Y.-H. Kim, S.-M. Han, W. Lee, M.-K. Han, Y. U. Lee, J.-I. Han, *Appl. Phys. Lett.* **2007**, *91*, 042113.
[30] V. Subramanian, P. C. Chang, J. B. Lee, S. E. Molesa, S. K. Volkman, *IEEE Trans. Components Packaging Technol.* **2005**, *28*, 742.
[31] P. Beecher, P. Servati, A. Rozhin, A. Colli, V. Scardaci, S. Pisana, T. Hasan, A. J. Flewitt, J. Robertson, G. W. Hsieh, F. M. Li, A. Nathan, A. C. Ferrari, W. I. Milne, *J. Appl. Phys.* **2007**, *102*, 043710.
[32] T. Shimoda, Y. Matsuki, M. Furusawa, T. Aoki, I. Yudasaka, H. Tanaka, H. Iwasawa, D. Wang, M. Miyasaka, Y. Takeuchi, *Nature* **2006**, *440*, 783.
[33] Y.-Y. Noh, X. Cheng, H. Sirringhaus, J. I. Sohn, M. E. Welland, D. J. Kang, *Appl. Phys. Lett.* **2007**, *91*, 043109.
[34] H. Cheong Min, S. Wagner, *IEEE Electron Device Lett.* **2000**, *21*, 384.
[35] Y. Wu, Y. Li, B. S. Ong, P. Liu, S. Gardner, B. Chiang, *Adv. Mater.* **2005**, *17*, 184.
[36] S. Molesa, D. Redinger, D. Huang, V. Subramanian, *Mater. Res. Soc. Symp. Proc.* (Eds: N. Fruehauf, B. R. Chalamala, B. E. Gnade, J. Jang), San Francisco **2003**, H8.3.1
[37] S. Gamerith, A. Klug, H. Scheiber, U. Schref, E. Moderegger, E. J. W. List, *Adv. Funct. Mater.* **2007**, *17*, 3111.
[38] W. S. Wong, E. M. Chow, R. Lujan, V. Geluz-Aguilar, M. L. Chabinyc, *Appl. Phys. Lett.* **2006**, *89*, 142118.
[39] J. Daniel, A. C. Arias, W. Wong, R. Lujan, S. Ready, B. Krusor, R. A. Street, *Jpn. J. Appl. Phys.* **2007**, *46*, 1363.
[40] M. L. Chabinyc, W. S. Wong, A. Salleo, K. E. Paul, R. A. Street, *Appl. Phys. Lett.* **2002**, *81*, 4260.
[41] T. Sekitani, Y. Noguchi, U. Zschieschang, H. Klauk, T. Someya, *Proc. Natl. Acad. Sci.* **2008**, *105*, 4976.
[42] Y. Noguchi, T. Sekitani, T. Yokota, T. Someya, *Appl. Phys. Lett.* **2008**, *93*, 043303.
[43] Y. R. Wu, M. Singh, J. Singh, *J. Appl. Phys.* **2003**, *94*, 5826.
[44] M. Singh, Y. R. Wu, J. Singh, *Solid-State Electron.* **2003**, *47*, 2155.
[45] W. J. Tseng, S. Y. Lin, S.-R. Wang, *J. Electroceram.* **2006**, *16*, 537.
[46] A. C. Arias, F. Endicott, R. A. Street, *Adv. Mater.* **2006**, *18*, 2900.
[47] T. X. Sun, G. E. Jabbour, *MRS Bull.* **2002**, 309.
[48] Y. Yoshioka, G. E. Jabbour, *Adv. Mater.* **2006**, *18*, 1307.
[49] E. Tekin, H. Wijlaars, E. Holder, D. A. M. Egbe, U. S. Schubert, *J. Mater. Chem.* **2006**, *16*, 4294.
[50] E. Tekin, P. J. Smith, S. Hoeppener, A. M. J. van den Berg, A. S. Susha, A. L. Rogach, J. Feldmann, U. S. Schubert, *Adv. Funct. Mater.* **2007**, *17*, 23.
[51] M. Singh, T. Kondou, H. Chae, J. D. Froehlich, S. Li, A. Mochizuki, G. E. Jabbour, *Mater. Res. Soc. Fall Meeting* **2008**, G13.7

[52] M. Singh, H. Chae, J. D. Froehlich, T. Kondou, S. Li, A. Mochizuki, G. E. Jabbour, *Soft Matter* **2009** DOI: 10.1039/B903531A.
[53] H. M. Haverinen, R. A. Myllylä, G. E. Jabbour, *Appl. Phys. Lett.* **2009**, *94*, 073108.
[54] S. Shigematsu, Y. Ishida, N. Nakashima, T. Asano, *Jpn. J. Appl. Phys.* **2008**, *47*, 5109.
[55] W. R. Small, F. Masdarolomoor, G. G. Wallace, M. in het Panhuis, *J. Mater. Chem.* **2007**, *17*, 4359.
[56] S. E. Shaheen, R. Radspinner, N. Peyghambarian, G. E. Jabbour, *Appl. Phys. Lett.* **2001**, *79*, 2996.
[57] V. Marin, E. Holder, M. M. Wienk, E. Tekin, D. Kozodaev, U. S. Schubert, *Macromol. Rapid Commun.* **2005**, *26*, 319.
[58] E. Holder, B. M. W. Langeveld, U. S. Schubert, *Adv. Mater.* **2005**, *17*, 1109.
[59] C. N. Hoth, S. A. Choulis, P. Schilinsky, C. J. Brabec, *Adv. Mater.* **2007**, *19*, 3973.
[60] T. Aernouts, T. Aleksandrov, C. Girotto, J. Genoe, J. Poortmans, *Appl. Phys. Lett.* **2008**, *92*, 033306.
[61] H.-W. Schock, R. Noufi, *Prog. Photovoltaics: Res. Appl.* **2000**, *8*, 151.
[62] M. A. Contreras, K. Ramanathan, J. AbuShama, F. Hasoon, D. L. Young, B. Egaas, R. Noufi, *Prog. Photovoltaics: Res. Appl.* **2005**, *13*, 209.
[63] O. Morton, *Nature* **2006**, *443*, 19.
[64] D. Cohen, *New Sci.* **2007**, 34.
[65] J. K. J. Van Duren, M. R. Robinson, C. Leidholm, *US Patent 20070163638*, **2007**.
[66] V. K. Kapur, M. Fisher, R. Roe, *Mater. Res. Soc. Symp. Proc.* **2001**, H2.6
[67] W. Voit, W. Zapka, L. Belova, K. V. Rao, *Proc. Sci. Meas. Technol.* **2003**, *150*, 252.
[68] Y. Li, C. Fu, J. Xu, *Jpn. J. Appl. Phys.* **2007**, *46*, 6807.
[69] T. H. van Osch, J. Perelaer, A. W. M. de Laat, U. S. Schubert, *Adv. Mater.* **2008**, *20*, 343.
[70] H. Meier, U. Löffelmann, D. Mager, P. J. Smith, J. G. Korvink, *Phys. Status Solidi A* **2009**, in press.
[71] N. Zhao, M. Chiesa, H. Sirringhaus, Y. Li, Y. Wu, B. Ong, *J. Appl. Phys.* **2007**, *101*, 064513.
[72] D. Huang, F. Liao, S. Molesa, D. Redinger, V. Subramanian, *J. Electrochem. Soc.* **2003**, *150*, G412.
[73] O. Ngamna, A. Morrin, A. J. Killard, S. E. Moulton, M. R. Smyth, G. G. Wallace, *Langmuir* **2007**, *23*, 8569.
[74] J. W. Song, C. S. Han, *Int. J. Precision Eng. Manuf.* **2008**, *9*, 79.
[75] J. W. Song, J. Kim, Y. H. Yoon, B. S. Choi, J. H. Kim, C. S. Han, *Nanotechnology* **2008**, *19*, 095702.
[76] T. Mustonen, K. Kordás, S. Saukko, G. Tóth, J. S. Penttilä, P. Helistö, H. Seppä, H. Jantunen, *Phys. Status Solidi B* **2007**, *244*, 4336.
[77] K. Kordás, T. Mustonen, T. Geza, H. Jantunen, M. Lajunen, C. Soldano, S. Talapatra, S. Kar, R. Vajtai, P. M. Ajayan, *Small* **2006**, *2*, 1021.
[78] L. Oyhenart, V. V. F. Demontoux, J. P. Parneix, *Microw. Opt. Technol. Lett.* **2005**, *44*, 460.
[79] M. Hiraoka, T. Hasegawa, Y. Abe, T. Yamada, Y. Tokura, H. Yamochi, G. Saito, T. Akutagawa, T. Nakamura, *Appl. Phys. Lett.* **2006**, *89*, 173504.
[80] K. Crowley, E. O'Malley, A. Morrin, M. R. Smyth, A. J. Killard, *Analyst* **2008**, *133*, 391.
[81] Y. Yoshioka, G. E. Jabbour, *Synth. Met.* **2006**, *156*, 779.
[82] J. Jang, J. Ha, J. Cho, *Adv. Mater.* **2007**, *19*, 1772.
[83] M. Börberl, M. V. Kovalenko, S. Gamerith, E. J. W. List, W. Heiss, *Adv. Mater.* **2007**, *19*, 3574.
[84] M. in het Panhuis, A. Heurtematte, W. R. Small, V. N. Paunov, *Soft Matter* **2007**, *3*, 840.
[85] A. Bietsch, J. Zhang, M. Hegner, H. P. Lang, C. Gerber, *Nanotechnology* **2004**, *15*, 873.
[86] S. Hauschild, U. Lipprandt, A. Rumplecker, U. Borchert, A. Rank, R. Schubert, F. Stephan, *Small* **2005**, *1*, 1177.
[87] S. N. Jayasinghe, A. N. Qureshi, P. A. M. Eagles, *Small* **2006**, *2*, 216.
[88] D. G. Yu, L.-M. Zhu, C. J. Branford-White, X. L. Yang, *J. Pharm. Sci.* **2008**, *97*, 3666.
[89] B. Derby, *J. Mater. Chem.* **2008**, *18*, 5717.
[90] R. C. Jaeger, *Introduction to Microelectronic Fabrication*, Vol. *5*, Addison-Wesley, Reading, MA, **1993**.
[91] T. Kawase, H. Sirringhaus, R. H. Friend, T. Shimoda, *Adv. Mater.* **2001**, *13*, 1601.
[92] Y. Xia, R. H. Friend, *Appl. Phys. Lett.* **2007**, *90*, 253513.
[93] B. J. de Gans, S. Hoeppener, U. S. Schubert, *J. Mater. Chem.* **2007**, *17*, 3045.
[94] S. M. Sze, *Semiconductor Devices: Physics and Technology*, John Wiley & Sons, New York **1985**.